Voronoi Diagrams and Perlin Noise for Simulation of Irregular Artefacts in Microscope Scans

Atef Alreni[1][a], Galina Momcheva[1,2][b] and Stoyan Pavlov[2,3][c]

[1]*Department of Computer Science, Varna Free University "Chernorizets Hrabar", Varna, Bulgaria*
[2]*Department of Advanced Computational Bioimaging, Medical University "Prof. Dr Paraskev Stoyanov", Varna, Bulgaria*
[3]*Department of Anatomy and Cell Biology, Medical University "Prof. Dr Paraskev Stoyanov", Varna, Bulgaria*

Keywords: Artefacts, Perlin Noise, Voronoi Diagrams, ANN.

Abstract: Artefacts are a common occurrence in microscopic images and scans used in life science research. The artefacts may be regular and irregular and arise from different sources: distortions of the illumination field, optical aberrations, foreign particles in the illumination and optical path, errors, irregularities during the processing and staining phases, et cetera. While several computational approaches for dealing with patterned distortions exist, there is no universal, efficient, reliable, and facile method for removing irregular artefacts. This leaves life scientists within cumbersome predicaments, wastes valuable time, and may alter the analysis results. In this article, the authors outline a systematic way to introduce synthetic irregular artefacts in microscopic scans via Perlin Noise and Voronoi Diagrams. The reasoning behind such a task is to produce pairs of "successful" and manufactured "failed" image counterparts to be used as training pairs in an artificial neural network tuned for artefact removal. At the moment, the outlined method only works for grayscale images.

SCITEPRESS SCIENCE AND TECHNOLOGY PUBLICATIONS

1 INTRODUCTION

Numerous differing sub-cellular structures can be mimicked via computation (Abdolhoseini, Kluge, Walker & Johnson, 2019). Various such approaches have recently been fathomed (for a thorough review, refer to (Ulman, Svoboda, Nykter, Kozubek & Ruusuvuori, 2016)). Within all these methods, two steps fall as being a commonality in all: firstly, the desired image is realised with objects of wanted number and shape, and secondly, background and foreground textures are created, which are later added to the respective ideal image to create a realistic noisy representation (Abdolhoseini et al., 2019).

Abdolhoseini et al. demonstrated a neuron image synthesiser in which Perlin noise (Perlin, 1985) and Gaussian mixture models (GMM (Reynolds, 2009)) were implemented, and akin characteristics in (Ulman et al., 2016) were utilized. Deformed elliptical shapes are created with spline interpolation (Unser, 1999) for single nuclei. Following this, foreground and background textures are created via Perlin noise (Perlin, 1985). Xiong et al. generated images of healthy Giemsa-stained red blood cell populations using deformation models and unbiased average shapes (Xiong, Wang, Ong, Lim & Jiang, 2010). Diffeomorphic demons (Vercauteren, Pennec, Perchant & Ayache, 2007), a non-parametric image registration, is used to deploy the model which maps one image to another. Successively, using histogram distribution models to conceive a proper texture, colour models were learned. Peng et al. (2009) applied an instance-based technique to model the shape space of 2D images of Hela cell nuclei using kernel distribution (Wasserman, 2004), but with this method, some of the simulated shapes do not match the original images, and the method requires large training datasets (Abdolhoseini, 2019).

Nonetheless, imaging artefacts vary in abstractness and reason for appearance. They mainly can be classified into three categories. Firstly, regularly patterned artefacts appear due to

[a] https://orcid.org/0000-0001-6548-8156
[b] https://orcid.org/0000-0003-0726-2022
[c] https://orcid.org/0000-0002-9322-2299

Alreni, A., Momcheva, G. and Pavlov, S.
Voronoi Diagrams and Perlin Noise for Simulation of Irregular Artefacts in Microscope Scans.
DOI: 10.5220/0010833000003123
In *Proceedings of the 15th International Joint Conference on Biomedical Engineering Systems and Technologies (BIOSTEC 2022) - Volume 2: BIOIMAGING*, pages 117-122
ISBN: 978-989-758-552-4; ISSN: 2184-4305

Copyright © 2022 by SCITEPRESS – Science and Technology Publications, Lda. All rights reserved

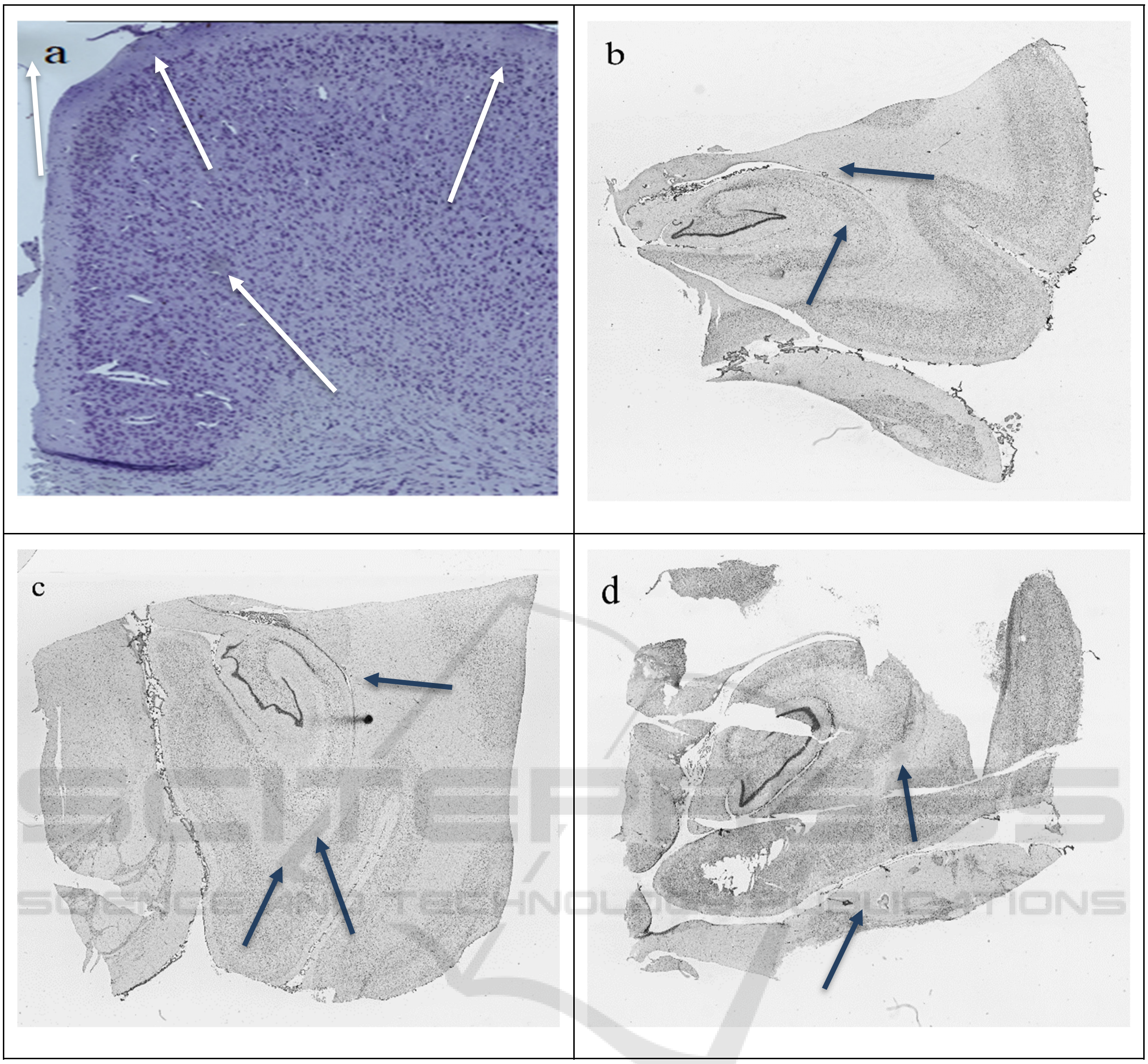

Figure 1: Examples of microscope scans with actual (arrowheads in a) and synthetically generated (arrowheads in b, c and d) artefacts. The artefacts in b, c and d are generated using the method described in Section 2.

SCITEPRESS SCIENCE AND TECHNOLOGY PUBLICATIONS

unevenness within the illumination field during scanning. The centre is brighter than the peripheral area around it (vignetting), which leads to a grid-like structure (seams) after the reconstruction. There are methods for removing this type of distortion; however, they either require recording the illumination field before the experiment or rely on computed estimates, leading to biases and errors in the result. Contrastingly, irregular artefacts (Figure 1a) have no method for reliable removal. They occur due to foreign particles or defects within the optical path, or form due to unstable tissue processing conditions, especially in areas with non-specific staining. These latter types are hard to predict and treat and are thus of most interest. The outlined innovative method for the generation of synthetic failed microscope scans focuses on imitating them.

In this paper, we utilise Perlin Noise and Voronoi diagrams through non-canonical means of original use for the sake of replicating the abstract shape and appearance of optical path artefacts in microscope scans. Subsequently, an aptly sized dataset, consisting of successful and unsuccessful microscope scans, can be produced due to both algorithms' mass versatility and leniency (their ability to have various parameters altered for specific desired outcomes). Generating such a dataset is paramount. The large dataset will be appropriate as input data to train a neural network to remove such artefacts in natural microscope scans. Thus, the authors have explored and identified a method for realising such artificial artefacts on microscope scans within this article. The rest of the article is organised as follows: Section 2 outlines the method in detail, Section 3 focuses on the results and their outcome, Section 4 highlights the technique's versatility and leniency, and Section 5 discusses the results' implications. A note of caution, in the subsequent paragraphs, a "cell" should be understood as "Voronoi cell" and not the biological entity.

2 METHOD

2.1 Voronoi Generation Mixed with Perlin Noise

Perlin noise and Voronoi diagrams have previously been used in parallel for achieving very concentrated and desired results (e.g., generating 3D digital phantoms of colon tissue (Svoboda, Homola & Stejskal, 2011) and generation of infinite virtual terrain, a common use case (Choros & Topolski, 2016)).

This step uses Voronoi diagrams, a data structure extensively investigated in computational geometry (Ferrero, 2011; Berg, Krevald, Overmars & Schwarzkopf, 1997), and Perlin noise, a type of gradient noise (Perlin, 1985; Bae, Kim, Kim, Park, Kim, Seo & Lee, 2018), coherently to create patches resembling image artefacts. The authors utilized Voronoi diagrams with the Euclidean distance calculating function. However, diverse desired results may be achieved using other distance metrics. A few additional parameters were deployed to aid in increasing the variance and prospect in results: these parameters are "noisiness", "excluded cells", and "desired cell(s)", where "noisiness" affects the noisiness of the Voronoi diagram (higher values results in smaller artefacts), "excluded cells" defines what parts of the Voronoi diagram will be removed and "desired cell(s)" defines what patch(es) will be used as the final artificial artefact(s).

Firstly, we define the number of cells (higher values produce better results but increase the number of computations), their locations (which are arbitrarily chosen) and an "excluded" value (a label with a value between 0 and 1, can be defined twice). The "desired cell(s)" value is defined later since potentially the "desired cell(s)" could be excluded if they are above, or below if "excluded cell(s)" is defined twice, the "excluded cell(s)" value. Also, the authors constrained the maximum and minimum value of each Voronoi cell's x and y coordinates to enhance efficacy, refer to Table 1 for more information.

Secondly, we iterate through each pixel within the image and identify the closest points to each cell through calculating their Euclidian distance as thus:

$$d(p,q)\ =\sqrt{\textstyle\sum_{i=0}^{n}}(q_i-\ p_i)^2 \tag{1}$$

where n defines the number of dimensions, and p and q represent the points within Euclidean space. Moreover, the closest points for the chosen cell are computed using the following formula:

$$R_k=\ \{x\ \in \boldsymbol{X}\,|\,d(x,P_k)\ \leq d(x,P_j)\ \forall\, j\ \neq k\} \tag{2}$$

such that X is a metric space with the distance function d, (2); K is a set of indices and (Pk) k∈K is a tuple of non-empty subsets within the space X; and Rk, which is associated with the site Pk, is the set of all points within X whose distance to Pk is not higher than their distance to the remaining sites Pj Such that j is any index that differs from k.

Thirdly, once the closest points are decided and each Voronoi cell is calculated, we normalise each distance value by dividing them by the maximum-distance value, allowing the distance values to range between 0 and 1. Following this, a "noisiness" value is generated (the value is a floating point number and ideally is below 2.0), then a Perlin noise value is generated for each pixel, which then is normalised to a value between 0 and 1 by dividing each value by 2 and adding 1.

Mathematically, Perlin noise is defined as:

$$p(x,y)=\ \sum_{i=0}^{n-1}\frac{\tilde{p}\,(\tilde{x},\tilde{y}\,)}{\gamma i},\ \ \tilde{x}=\ \beta^i x,\ \tilde{y}=\ \beta^i y \tag{3}$$

where n defines the number of wanted 'octaves', p(.) represents a simple Perlin noise function defined by Perlin (1985), γ and β are parameters that regulate and control the octave magnitude and noise smoothness. The higher β is, the less smooth is the noise (1), refer to Table 1.

Fourthly, we combine each normalised distance value with its respective Perlin noise value and the noisiness value through utilisation of equation (4):

$$f\ =\ v+(n*p) \tag{4}$$

where v is the normalised distance value, n is the noisiness parameter and p is the generated and normalised Perlin noise value, refer to Table 1.

SCIENCE AND TECHNOLOGY PUBLICATIONS

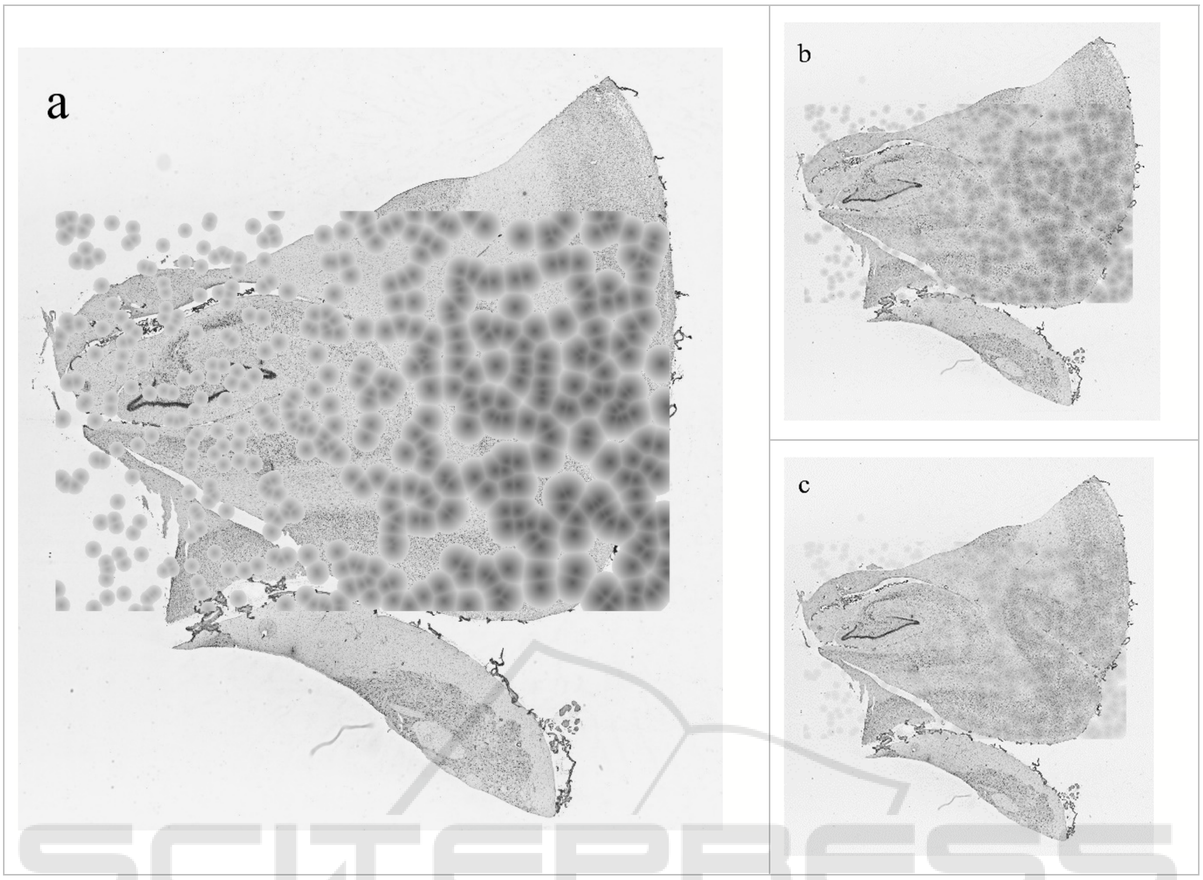

Figure 2: Examples of images produced in the intermediate steps of the algorithm: a. Result of 2.1; b. Result of 2.2; c. Result of 2.2 after repetition.

SCITEPRESS SCIENCE AND TECHNOLOGY PUBLICATIONS

Finally, we exclude all the undesired cells by checking whether their final normalised value is ≥ “excluded cell(s)” (excluded if the expression evaluates to TRUE). In this article, cells that were too light, i.e., cells which have become non-visible and/or do not resemble the shading of a natural artefact were removed. The “excluded cell(s)” value allows the programmer to control the accepted shading of their artefact. Therefore, the criterion for estimating if a cell is excluded can be manipulated, depending on the desired outcome: if too light and dark artefacts are not desired, then normalised values ≥ “excluded cell(s)” value one and normalised values ≤ “excluded cell(s)” value two will be excluded. Then, we multiply all the non- removed cells’ final distance values by 255 and set each Voronoi cell’s pixel value to the final result, respectively. Also, a “desired cell(s)” value (which is between 1 and the number of cells, excluding any cells that have been removed) is generated and it will determine what cell(s) will be used as the final artefact(s). In the examples used in this article, the “desired cell(s)” value was manually chosen, but it can be assigned randomly.

2.2 Blended (Optionally Can Be Repeated)

Within this step, we merge the original successful microscope scan with the image generated in ***2.1.*** This allows an image with lighter Voronoi cells, which fade naturally into the image to be generated. This is essential as the periphery of actual artefacts shows similar seamless fading into the microscope scan. Moreover, the central color of the artefact is lightened as well, which is vital as ideally the artefact should not be too dark.

Both images are combined using equation (5):

$$m(A,B) = \frac{1}{2}A + \frac{1}{2}B \quad (5)$$

where A represents a two-dimensional matrix of the pixel values of the successful microscope scan, and B represents a two-dimensional matrix of the pixel values of the image from ***2.2***.

Table 1. Parameters used to generate the synthetic failed microscope scan demonstrated in Figure 1b.

Perlin noise	**n**	$\boldsymbol{\gamma}$	$\boldsymbol{\beta}$	**scale**	**Other parameters (Voronoi)**
2.1	5	0.5	2.0	(image width, image height)	C = 500, CL = random (x = 112-1957, y = 712-1877), EC = 0.85, DC = 183 & 186

Discretionally, this step can be repeated where the newly blended image from this step is blended again with the original successful microscope scan, depending on what type of artefacts are wanted. If the programmer wants to generate lighter artefacts that are more subtle in appearance, then this step should be repeated to achieve such an artefact. The authors have repeated this step to illustrate what artefacts are generated from such an approach (Figure 1a). Figure 1d shows artefacts from only one iteration of this step; they are darker and more visible, generally the better approach in most cases.

2.3 Extrapolation

Finally, for the final result generation, we use the "desired cell(s)" parameter, defined in 2.1, to extract the wanted cells from the image generated in 2.3 onto the successful microscope used initially. Specifically, this is achieved by iterating over the Voronoi section of the image from 2.3 and checking whether it is part of the desired cell(s). If it is, we alter the pixel value of the original image to that of the one from 2.3. Upon completion artefacts analogous to those in Figure 1b are created, depending on what values were inputted for the parameters and if 2.2 was repeated. Artefacts in Figure 1c and 1d were generated without repetition of 2.2.

3 RESULTS

The described algorithm generates a synthetic artefact(s) on a successful microscope scan, as shown in "Figure 1b and 1c". The perceptual similarity between both artefacts, artificial and "natural", pertaining to human-eye estimation, is high and desirable: the artefacts synthetically generated within Figure 1b, 1c and 1d naturally blend into the image without seeming far too artificial, i.e., a massive colour-contrast difference between the exterior of the artefact and the pixels around it, is not present, allowing the artefact to fade into the image and to seem non-artificial. Also, the artefact(s) is aptly sized and has the necessary shaping mechanism. The method does not force the artefact(s) to be specifically shaped; therefore, with every artefact a somewhat abstract/realistic shape can be generated, as seen in Figure 1b and 1c. This proves to be useful as actual artefacts cannot be identified as having specific shapes. Moreover, the locations and quantity of artefacts can be controlled, meaning one successful input image can be utilised to generate numerous successful microscope scans with artificial artefacts. Also, artefacts of distinctive shade can be generated through repetition or non-repetition of step 2.2, as seen in Figure 1b when compared to Figure 1c and 1d.

4 VERSATILITY & LENIENCY

The potency laid in a programmer's hand regarding achievable artefacts via the authors' method is immense, since the method supplies the programmer with various parameters that can be altered for attaining specific results, depending on what is desired. For instance, the Perlin noise function (Perlin, 1985) has over six parameters and directly affects the size and shade of artefacts, enabling the programmer to alter the respective Perlin noise parameters to achieve lighter artefacts with smother transitions or darker artefacts with less-smooth transitions.

Furthermore, by manipulating the number of Voronoi cells the programmer can alter effectively the shape and size of the generated artefacts. The function used for calculating the distance between Voronoi points can be altered as numerous distance-calculation functions exist (e.g., Euclidean (Gomathi & Karthikeyan, 2014; Ranjitkar & Karki, 2016) and Manhatton distance (Gomathi & Karthikeyan, 2014; Ranjitkar & Karki, 2016)). This enables further manipulation opportunities for the programmer; the noisiness parameter allows to increase the roundness of each artefact and their size, which proves to be as artefacts vary in roundness and size.

Lastly, the parameters ‘excluded cell(s)’ and ‘desired cell(s)’ allow the programmer to deduct a chosen proportion of cells. This controls the generation of certain types of artefacts (lighter artefacts, darker artefacts or artefacts of generic shade). Visually appropriate cells can be selected manually or automatically. The latter increases the speed of artificial-failed microscope scan generation.

5 CONCLUSION

Within this article, the authors have described a method for synthetic generation of “failed” microscope scans for later use as augmented input data within a neural network. The method outlined within this article is promising as the generated and the actual artefacts are very similar in visual appearance. The artificial image distortions created with this method naturally blend in microscope scans. Furthermore, the method is easy to use and is exceptionally versatile and lenient, i.e., it provides the programmer with numerous parameters which all can be slightly or massively tweaked to achieve distinctive results. Finally, due to the method’s versatility and leniency, it can synthetically generate numerous “failed” microscope scans by only being provided with one successful microscope scan, allowing massive datasets to be produced for training an artificial neural network to eliminate these tiresome artefacts.

Although the quandaries above are intimidating to the approach regarding restoration, the authors within this article have developed and outlined the foundation for solving this reoccurring and unabating problem. The final solution will be achieved through using a dataset generated from collecting numerous and various successful microscope scans and their synthetically generated failed counterparts, using the method described within this article.

REFERENCES

Abdolhoseini, M., Kluge, M.G., Walker, F.R., & Johnson, S.J. (2019). Neuron Image Synthesizer Via Gaussian Mixture Model and Perlin Noise. *2019 IEEE 16th International Symposium on Biomedical Imaging (ISBI 2019),* 530-533. doi: 10.1109/ISBI.2019.8759471

Bae, H.J., Kim, C.W., Kim, N., Park, B., Kim, N., Seo, J.B., & Lee, S.M. (2018). A Perlin Noise-Based Augmentation Strategy for Deep Learning with Small Data Samples of HRCT Images. *Scientific Reports, 8*(1). doi: 10.1038/s41598-018-36047-2

Berg, M.D., Cheong, O., Kreveld, M.V., Overmars, M., & Schwarzkopf, O. (1997). Computational Geometry: Algorithms and Applications. Springer-Verlag.

Choros, K., & Topolski, J. (2016). Parameterized and Dynamic Generation of an Infinite Virtual Terrain with Various Biomes using Extended Voronoi Diagram. *J. Univers. Comput. Sci., 22*, 836-855.

Ferrero, M.M.A. (2011). Voronoi Diagram: The Generator Recognition Problem. *Computing Research Repository - CORR*.

Gomathi, V.V., & Karthikeyan, S. (2014). Performance Analysis of Distance Measures for Computer tomography Image Segmentation.

Peng, T., Wang, W., Rohde, G.K., & Murphy, R.F. (2009). Instance-Based Generative Biological Shape Modeling. Proceedings. *IEEE International Symposium on Biomedical Imaging, 5193141*, 690–693. doi: 10.1109/ISBI.2009.5193141

Perlin, K. (1985). An image synthesiser. *SIGGRAPH Comput. Graph., 19*, 287-296. doi: 10.1145/325165.325247

Ranjitkar, H.S., & Karki, S. (2016). Comparison of A*, Euclidean and Manhattan distance using Influence map in MS. Pac-Man.

Reynolds, D. (2009). *Gaussian Mixture Models*. In: Li, S.Z. & Jain, A. (eds.) Encyclopedia of Biometrics. Springer, Boston, MA. doi: 10.1007/978-0-387-73003-5_196

Svoboda, D., Homola, O., & Stejskal, S. (2011). Generation of 3D Digital Phantoms of Colon Tissue. In: Kamel, M. & Campilho, A. (eds.) Image Analysis and Recognition. ICIAR 2011. *Lecture Notes in Computer Science, 6754*. Springer, Berlin, Heidelberg. doi: 10.1007/978-3-642-21596-4_4

Ulman, V., Svoboda, D., Nykter, M., Kozubek, M., & Ruusuvuori, P. (2016). Virtual cell imaging: A review on simulation methods employed in image cytometry. *Cytometry Part A, 89*(12), 1057-1072. doi: 10.1002/cyto.a.23031

Unser, M. (1999). Splines: a perfect fit for signal and image processing. *IEEE Signal processing Magazine, 16*(6), 22-38. doi: 10.1109/79.799930

Vercauteren, T., Pennec, X., Perchant, A., & Ayache, N. (2007). Non-parametric diffeomorphic image registration with the demons algorithm. *Medical image computing and computer-assisted intervention: MICCAI ... International Conference on Medical Image Computing and Computer-Assisted Intervention, 10*(Pt 2), 319–326. doi: 10.1007/978-3-540-75759-7_39

Wasserman, L. (2004). *All of Statistics: A Concise Course in Statistical Inference*. Springer, New York, NY. doi: 10.1007/978-0-387-21736-9

Xiong, W., Wang, Y., Ong, S.H., Lim, J.H., & Jiang, L. (2010). Learning cell geometry models for cell image simulation: An unbiased approach. *2010 IEEE International Conference on Image Processing*, 1897-1900. doi: 10.1109/ICIP.2010.5652455

SCITEPRESS SCIENCE AND TECHNOLOGY PUBLICATIONS